ACS APPLIED MATERIALS & INTERFACES

www.acsami.org

Research Article

Bioinspired Electro-RAFT Polymerization for Electrochemical Sensing of Nucleic Acids

Qiong Hu,* Yilin Luo, Xiaojing Cao, Zhuohua Chen, Yanyu Huang, and Li Niu*

Cite This: *ACS Appl. Mater. Interfaces* 2021, 13, 54794−54800

Read Online

ACCESS | Metrics & More | Article Recommendations | Supporting Information

ABSTRACT: Sensing of ultralow-abundance nucleic acids (NAs) is integral to medical diagnostics and pathogen screening. We present herein an electrochemical method for the highly selective and amplified sensing of NAs, using a peptide nucleic acid (PNA) recognition probe and a bioinspired electro-RAFT polymerization (BERP)-based amplification strategy. The presented method is based on the recognition of target NAs by end-tethered PNA probes, the labeling of thiocarbonylthio reversible addition−fragmentation chain transfer (RAFT) agents, and the BERP-assisted growth of ferrocenyl polymers. The dynamic growth of polymers is electrochemically regulated by the reduction of 1-methylnicotinamide (MNA) organic cations, the redox center of nicotinamide adenine dinucleotide (NAD^+, coenzyme I). Specifically, electroreduction of the MNA cations causes the fragmentation of thiocarbonylthio RAFT agents into radical species, triggering the polymerization of ferrocenyl monomers, thereby recruiting plenty of ferrocene electroactive tags for amplified sensing. It is obvious that the BERP-based strategy is inexpensive and simple in operation. Benefiting from the high specificity of the PNA recognition probe and the amplified signal by the BERP-based strategy, this method is highly selective and the detection limit is as low as 0.58 fM (S/N = 3). Besides, it is applicable to the sensing of NAs in serum samples, thus showing great promise in the selective and amplified sensing of NAs.

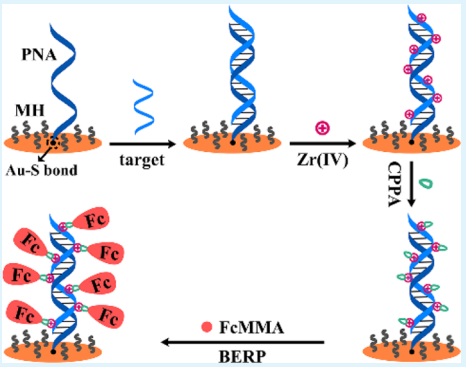

KEYWORDS: *electrochemical biosensor, nucleic acid, bioinspired polymerization, redox mediator, peptide nucleic acid, electro-RAFT polymerization*

1. INTRODUCTION

Selective and amplified sensing of nucleic acids (NAs) is greatly important to the clinical screening of potential markers (e.g., microRNA (miRNA) and circulating tumor DNA (ctDNA)), the early diagnosis of malignant tumors and genetic diseases (e.g., breast cancer and congenital deafness), the identification and screening of pathogens (e.g., *Aspergillus flavus* and COVID-19), etc. During the past few decades, various methods have been presented for the amplified sensing of NAs[1−8] using, for example, functional nanomaterials,[9−11] enzymes,[12−15] and polymers for signal amplification.[16−19] Among them, the use of polymers for amplified sensing of NAs is impressive[20−23] because of their low cost, undemanding experimental conditions, simplicity in operation, and superior chemical/thermal stability.[16] On the basis of the electrostatic labeling of ferrocene (Fc)-functionalized cationic polythiophenes, Le Floch et al.[18] presented an electrochemical method for the amplified sensing of NAs using a peptide nucleic acid (PNA) recognition probe. This method is simple in operation and inexpensive. However, the direct labeling of preformed polymers for amplified sensing suffers from the intrinsic defects of low labeling efficiency and a limited labeling amount of polymer chains because the diffusion of bulky and curly polymer chains from a solution to labeling sites is kinetically and sterically disfavored.[21] To further bypass these two defects, great effort has recently been devoted to developing methods based on the controlled growth of polymers from the labeling sites.[17,19] Compared with the direct labeling of polymers for amplified sensing, this approach holds the advantages of higher labeling efficiency and an improved labeling amount of polymer chains.[16,21] Through the growth of polymer spots by reversible addition−fragmentation chain transfer (RAFT) polymerization of methacrylate monomers, He et al. presented a visual method for the amplified sensing of NAs fewer than 2000 copies.[20]

As a well-established reversible deactivation radical polymerization (RDRP) technique, RAFT polymerization is known to be regulated by thiocarbonylthio (S = C(Z)S-R) RFAT agents via a typical degenerative chain transfer mechanism.[24−26] Since its discovery by Chiefari et al.,[25] it has attracted growing attention in the controlled synthesis of polymers with well-

Received: September 12, 2021
Accepted: October 26, 2021
Published: November 9, 2021

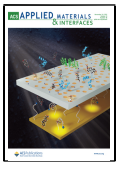

https://doi.org/10.1021/acsami.1c17564
ACS Appl. Mater. Interfaces 2021, 13, 54794−54800

defined architectures and molecular weights.[24,27] In a RAFT process, the initiating radicals are conventionally supplied by thermal activation of the radical initiators.[20,28] For milder reaction conditions and avoiding the thermal decomposition of heat-liable components, recent research interest has focused on alternative means to initiation by other external stimuli, such as enzymatic,[29] photochemical,[30] mechanical,[31] and electrochemical methods.[32−34] Among them, electrochemical stimuli (i.e., potential and current) offer the benefits of mild reaction conditions (i.e., at room temperature) and improved control over the polymerization process.[34−36] However, there are only a few successful examples concerning electro-RAFT polymerization because it requires the use of suitable redox mediators to shuttle electrons from the electrode interface to RAFT agents to invoke the generation of initiating and propagating radicals.[36,37] Using nicotinamide adenine dinucleotide (NAD^+, coenzyme I (CoI)) as the mediator, Sang et al. reported an interesting example of electro-RAFT polymerization.[37] In this method, electroreduction of CoI causes the fragmentation of the RFAT agent to yield a radical species, thereby initiating the growth of polymers with targeted molecular weight, good chain-end fidelity, and low dispersity. For the CoI mediator, the features of rapid electron transfer, mild redox ability, and reversible redox states are quite appealing. Nevertheless, its high cost and poor stability are adverse to potential applications. For nicotinamide-based electron carriers (e.g., NAD^+/NADH and $NADP^+$/NADPH) in most enzymatic oxidation−reduction reactions (e.g., the electron transport chain), the redox reaction typically takes place at the N-substituted pyridinium ring.[38,39] Inspired by this fact, we extrapolate that it is able to realize the electro-RAFT polymerization using other nicotinamide derivatives with a pyridinium center (e.g., 1-methylnicotinamide (MNA)) as redox mediators.

On the basis of the bioinspired electro-RAFT polymerization (BERP)-assisted growth of polymers using the MNA organic cation as the redox mediator, we present herein a novel electrochemical method for the amplified sensing of NAs. As the redox center of CoI, the MNA cation offers the advantages of low cost and superior stability. The principle of this method is illustrated in Scheme 1. The PNA probe, which is end-tethered by the formation of a gold−sulfur (Au−S) bond, is used to specifically recognize the target NA. In addition to the merits of superior specificity and high resistance to enzymatic hydrolysis, the uncharged *N*-(2-aminoethyl)glycine (2-AEG) backbone of the PNA probe endows the hybridized heteroduplexes with minimal ionic strength dependence, improved hybridization efficiency, and superior thermal stability.[40] After hybridization, the phosphate sites of the target NAs are used for the subsequent complexation of 4-cyano-4-(phenylcarbonothioylthio)pentanoic acid (CPPA) agents (serving as RAFT agents) via phosphate-Zr(IV)-carboxylate (PZC) chemistry, which is highly efficient, robust, simple in operation, and inexpensive.[21,41] Then, the BERP-assisted growth of polymers under mild conditions would recruit plenty of Fc tags for amplified sensing. As a result, this method is highly selective and sensitive toward the electrochemical sensing of NAs. In addition, it can be applied to the sensing of NAs in complex serum samples, thus holding great potential in practical applications.

Scheme 1. BERP-Based Electrochemical Sensing of Nucleic Acids

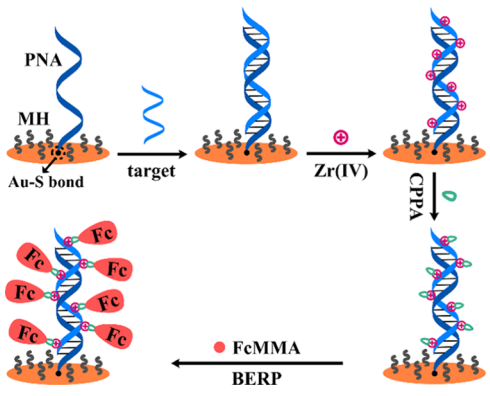

2. EXPERIMENTAL SECTION

2.1. Materials and Reagents. The PNA recognition probe and HPLC-purified NAs were supplied by Allpeptide Biotechnology Co., Ltd. (Hangzhou, China) and Sangon Biotech (Shanghai) Co., Ltd. (Shanghai, China), respectively. Their sequences are given as follows

The PNA recognition probe: 5′-HS-$(CH_2)_{11}$-G ATT TTC TTC CTT TTG TTC-3′.

The target fragment (target): 5′-G AAC AAA AGG AAG AAA ATC-3′.

The single-site mismatched fragment (SSM): 5′-G AAC AAA AGC AAG AAA ATC-3′.

The three-site mismatched fragment (TSM): 5′-G AAT AAA AGC AAG AAT ATC-3′.

The noncomplementary fragment (NC): 5′-A CTT CCG TAC TTA GTT GAA-3′.

MNA, *N*,*N*-dimethylformamide (DMF), $LiClO_4$, $K_3Fe(CN)_6$, absolute ethanol, normal human serum (NHS), and ferrocenylmethyl methacrylate (FcMMA) were offered by TCI (Shanghai) Development Co., Ltd. (Shanghai, China), Macklin Biochemical Co., Ltd. (Shanghai, China), Aladdin Biochemical Technology Co., Ltd. (Shanghai, China), Damao Chemical Reagent Factory (Tianjin, China), Sinopharm Chemical Reagent Co., Ltd. (Shanghai, China), YiJi Industries Co., Ltd. (Shanghai, China), and FDC Chemical (Shanghai, China), respectively. 6-Mercapto-1-hexanol (MH), $ZrOCl_2$, and CPPA were collected from Sigma-Aldrich (Shanghai, China). KPF_6 and $K_4Fe(CN)_6$ were provided by J&K Scientific Ltd. (Shanghai, China). Ultrapure water (≥18.25 MΩ cm) was used as the water source.

Phosphate-buffered solution (PBS, pH 7.4) was prepared by appropriately mixing 10 mM Na_2HPO_4 with 10 mM NaH_2PO_4. The solution for BERP was obtained by sequentially adding 3.0−7.5 μL of MNA (10 mM), 0.5 mL of the FcMMA monomer (10 mM in DMF), and 7.5 mL of KPF_6 (0.1 M) into 2 mL of DMF. The solution for potentiostatic impedance tests was 5 mM $Fe(CN)_6^{3-/4-}$ in 0.1 M KNO_3.

2.2. Apparatus. Cyclic voltammetry (CV), *i*−*t* curve, and square-wave voltammetry (SWV; quiet time, 15 s; potential increase, 4 mV; frequency, 15 Hz; potential amplitude, 25 mV) were tested on a CHI760E electrochemical workstation (CH Instruments). Nyquist plots were collected with a potential amplitude of 5 mV at an open-circuit voltage of ∼0.19 V from 0.1 MHz to 0.1 Hz with a Reference 600 Plus potentiostat (Gamry Instruments). All these tests were carried out at room temperature, using a 3 mm gold (Au) working electrode, a saturated calomel reference electrode (SCE), and a Pt wire counter electrode. Morphologic analysis was conducted at an accelerating voltage of 15 kV with a JSM-7100F field emission scanning electron microscope (SEM, JEOL).

2.3. BERP-Based Electrochemical Sensing of NAs. After the sequential pretreatment according to the previous report,[33] a cleaned Au electrode was incubated at 37 °C with 7.5 μL of the PNA recognition probe (0.5 μM) for 0.5 h. After soaking the Au/PNA

https://doi.org/10.1021/acsami.1c17564
ACS Appl. Mater. Interfaces 2021, 13, 54794−54800

electrode at 37 °C in 1 mM MH (60% ethanol) for 0.25 h, the Au/PNA/MH electrode was rinsed with ethanol and ultrapure water. Further, it was incubated at 37 °C with 10 μL of NAs (10 mM PBS) for 1 h. Following the rinsing with copious ultrapure water, the Au/PNA/MH/NA electrode was soaked at 37 °C in 2.5 mM $ZrOCl_2$ (20% EtOH) for 0.25 h. The obtained Au/PNA/MH/NA/Zr electrode was thoroughly rinsed with ultrapure water, soaked at 37 °C in 0.5 mM CPPA (20% ethanol) for 0.25 h, and rinsed sequentially with ethanol and ultrapure water. Then, the Au/PNA/MH/NA/Zr/CPPA electrode was immersed in the solution for BERP (stirred moderately), followed by the running of the *i*−*t* curve for another 1.5 h. Last, the Au/PNA/MH/NA/Zr/CPPA/Fc electrode was thoroughly rinsed with ethanol and ultrapure water and measured by SWV in 0.5 M $LiClO_4$.

3. RESULTS AND DISCUSSION

3.1. Principle of the BERP-Based Electrochemical Sensing of NAs. Similar to CoI, the pyridinium center of the MNA organic cation can accept an electron from the electrode to form an organic radical, as shown in Figure S1.[38,39] Further, the organic radical can efficiently reduce the thiocarbonylthio RAFT agent (S = C(Z)S-R) to yield a radical ($R^•$) and an anionic fragment (S = C(Z)S^-),[35] while itself is oxidized back into the initial cationic form.[33,36] That is, the MNA organic cations act as redox mediators to shuttle electrons from the electrode interface to reduce the RAFT agents, which subsequently fragment to yield the $R^•$ initiating radicals.[36] As the CPPA RAFT agents are tethered to the electrode via the R-group, the resulting $R^•$ radicals are tethered to the electrode interface as well.[41] The surface-tethered $R^•$ radicals can react continuously with numerous ferrocenyl monomers,[41] leading to the dynamic growth of polymers,[32] thereby recruiting plenty of Fc electroactive tags for amplified sensing.[32,33]

3.2. Redox Properties of the MNA Cation and the CPPA Agent. BERP is mediated by the electroreduction of the MNA organic cations. Previous reports disclosed that the RAFT agents can be electrochemically cleaved at the C−S bond to form two fragments that would be further reduced to carbanions,[34,35] which are unable to (re)initiate or sustain the polymerization process. In fact, it has been found that the direct application of electrochemical stimuli to a system containing RAFT agents and vinyl monomers did not yield any polymer.[35] To avoid the direct electroreduction of RAFT agents, the prerequisite is that the electroreduction of the externally added mediators should take place at a potential significantly higher than the reduction potential of the corresponding RAFT agent.[41] To demonstrate the suitability of using the MNA cation as a surrogate of the CoI mediator in regulating the electro-RAFT polymerization, cyclic voltammograms (CVs) of MNA and CPPA were collected to probe their respective redox waveforms (Figure 1). The CV of MNA features two reduction peaks, corresponding to the formation of an organic radical (−0.36 V) and a dihydropyridine species (−0.6 V).[33,38] As the peak potential corresponding to the one-electron reduction of CoI is located at −0.75 V,[33] the use of the MNA organic cation as the mediator holds the advantage of milder reduction potential. The CV of CPPA features a reduction peak at −1.02 V.[32] As the reduction potential corresponding to the electrogeneration of the organic radical is significantly higher (by about 0.66 V) than that of the CPPA agent, the electroreduction of the MNA cations would not be accompanied by the irreversible consumption of the CPPA agents. Therefore, it is able to perform electro-RAFT polymerization using the MNA organic cation as the mediator.

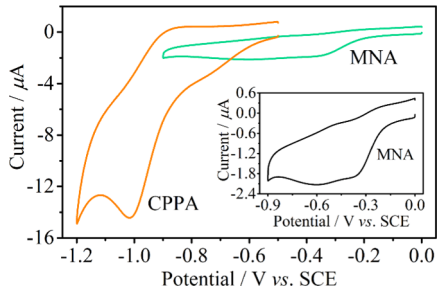

Figure 1. CVs of MNA and CPPA. MNA, 1 mM; CPPA, 1 mM; and the supporting electrolyte is an N_2-saturated 1:1 (v/v) mixture of 0.1 M KPF_6 and DMF.

3.3. Effects of Experimental Conditions. The BERP is regulated by the electroreduction of the MNA cations. For controlled polymerization, the concentration of radicals (including the initiating and propagating ones) should be sufficiently low to limit the undesired radical dimerization, but the high polymerization efficiency requires the supply of sufficient radicals.[32] As a result, the growth kinetics of polymers is highly dependent on the concentration of MNA and the reduction potential. As shown in Figure S2, the CV of the MNA cation at the Au/PNA/MH/NA/Zr/CPPA electrode features a reduction peak at about −0.5 V. According to this observation, the effect of MNA concentration on the peak current (corresponding to the oxidation of Fc tags) was investigated at an electroreduction potential of −0.5 V. As shown in Figure 2A, the highest peak current appears at a

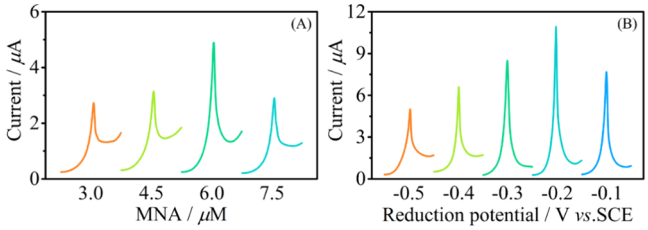

Figure 2. (A) Effect of MNA concentration. Target, 1 nM and reduction potential, −0.5 V. (B) Effect of reduction potential. Target, 1 nM.

MNA concentration of 6 μM. This trend is in expectation because the further increase of MNA concentration would result in the generation of a higher concentration of organic radicals, leading to the undesired radical termination.[32] Further, the effect of reduction potential on the peak current was studied (Figure 2B). The peak current is found to increase with the increase of reduction potential from −0.5 to −0.2 V and then decreases with the further increase of reduction potential. Thus, the optimal reduction potential is −0.2 V. This can be ascribed to the fact that a more negative reduction potential corresponds to the exacerbation of radical termination,[32] while a lower concentration of organic radical at a more positive reduction potential would result in a lower polymerization efficiency. Hence, optimal conditions were applied for the subsequent experiments.

3.4. Characterization of the Modified Electrodes. The reliability of the electrochemical signal was evaluated based on the control experiments (Figure 3A). The square-wave voltammogram (SWV) of the perfectly modified Au/PNA/MH/NA/Zr/CPPA/Fc electrode features a high oxidation

https://doi.org/10.1021/acsami.1c17564
ACS Appl. Mater. Interfaces 2021, 13, 54794−54800

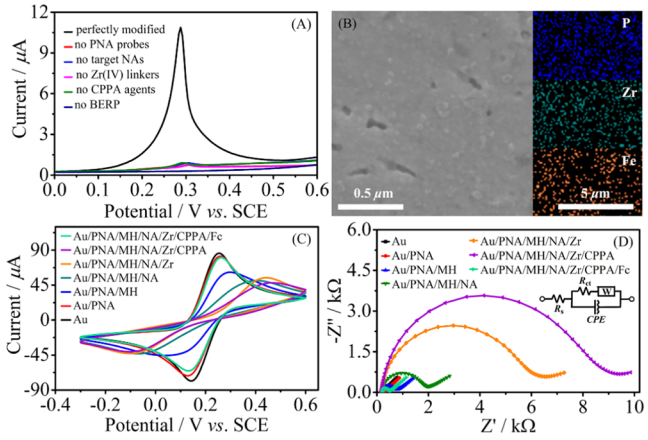

Figure 3. (A) SWVs of differently modified Au electrodes. (B) SEM image and elemental mappings of the Au/PNA/MH/NA/Zr/CPPA/Fc electrode. (C) CVs and (D) Nyquist plots of the stepwise modified Au electrodes. In the inset equivalent circuit, R_s, R_{ct}, W, and CPE represent the solution resistance, charge-transfer resistance, Warburg resistance, and constant-phase element, respectively. Target, 1 nM.

peak at 0.29 V, corresponding to the one-electron oxidation of the Fc tags.[21,33] For the control experiments conducted without PNA recognition probes, target NAs, Zr(IV) linkers, CPPA agents, or BERP, no clear oxidation peak appears. Therefore, the electrochemical signal is reliable for the sensing of NAs. Besides, CVs of the Au/PNA/MH/NA/Zr/CPPA/Fc electrode (Figure S3) show that the peak currents are linear to the scan rate, indicating the tethering of the Fc electroactive tags onto the electrode.[21,28]

As observed, there are numerous polymers on the Au/PNA/MH/NA/Zr/CPPA/Fc electrode (Figure 3B), indicating the high efficiency of the BERP-based strategy. Further, the presence of target NAs, Zr(IV) linkers, and Fc electroactive tags on the Au/PNA/MH/NA/Zr/CPPA/Fc electrode was evidenced by the elemental traces of P, Zr, and Fe, respectively.

CVs and impedance spectra were applied to track the stepwise modification process of the electrodes. Figure 3C,D shows the representative CVs and Nyquist plots, respectively. The CV of the Au electrode is featured by a couple of reversible waveforms, while the charge-transfer resistance (R_{ct}) is as low as ~35 Ω. The modification with PNA recognition probes downregulates the peak currents, and the R_{ct} value increases to ~120 Ω. Similar trends are observed for the modification with MH agents (R_{ct}, ~610 Ω). These are caused by the steric hindrance.[21] Due to the presence of steric hindrance and electrostatic repulsion,[32] the introduction of target NAs further downregulates the peak currents, and the R_{ct} value increases to ~1.80 kΩ. The modifications with Zr(IV) linkers and CPPA agents greatly downregulate the peak currents, and the R_{ct} value increases to ~6.3 and ~9.2 kΩ, respectively; these trends are in line with previous observations.[21,33] Impressively, the BERP greatly upregulates the peak currents, and the R_{ct} value decreases to ~340 Ω. This is in expectation because the presence of plenty of Fc tags can greatly facilitate the charge transfer.[33] As can be seen, the trend in the current change agrees with that of the R_{ct} value. Taking together, the modification process of the electrodes is successful.

3.5. Analytical Performance. Under optimal conditions, the concentration-dependent SWVs were collected, as shown in Figure 4. A higher peak current can be observed at a higher

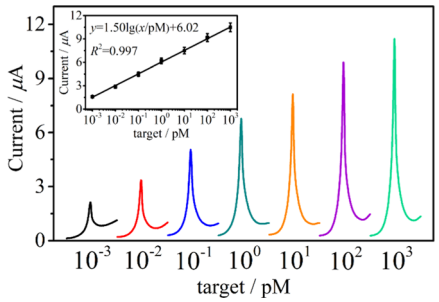

Figure 4. Concentration-dependent SWVs. The inset shows the calibration plot of peak current versus target concentration. Error bars correspond to standard deviations (n = 5).

target concentration. Thus, this method allows for the signal-on sensing of NAs, which is less susceptible to false positives. This is in expectation because more target NAs could result in the labeling of more Fc electroactive tags. Furthermore, the peak current is observed to be linear to the logarithm of target concentration over a sensing range from 1 fM to 1 nM. The regression equation is $y = 1.50\,\lg(x/\mathrm{pM}) + 6.02$ ($R^2 = 0.997$), with a detection limit of 0.58 fM (S/N = 3). The detection limit is lower than those of most of the previous sensing methods (Table S1), including fluorescence,[11,42−44] electrochemiluminescence (ECL),[45] electrochemical,[46−49] photoelectrochemical (PEC),[50,51] etc. To a significant extent, the improved sensitivity of this method can be ascribed to the signal amplification by the BERP-based strategy. As the coefficients of variation (n = 5) corresponding to the intra- and inter-sensing of a 1 nM target are 5.6 and 5.9%, respectively, the sensing reproducibility of this method is satisfactory. After 2-week storage at 4 °C, the peak current toward the 1 nM target can be retained by about 94.2%, indicating that the storage stability is acceptable.

3.6. Selectivity and Practicability. The selectivity (or specificity) of this method was studied based on the sensing of four different NAs, including target, SSM, TSM, and NC fragments. The presence of a single-site mismatch would result in a decrease of the peak current by ~70.7% (Figure 5A),

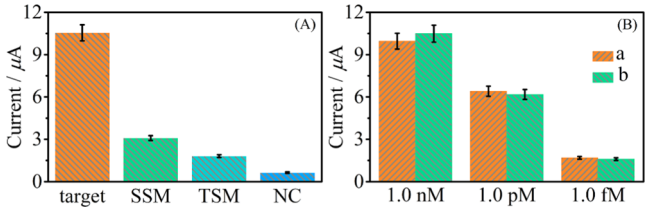

Figure 5. (A) Peak currents toward four NA fragments (1 nM). (B) Peak currents toward samples (a) with and (b) without 10% serum matrices. Error bars correspond to standard deviations (n = 5).

indicating that this method is capable of sensing single-nucleotide polymorphism. For the TSM and NC fragments, the peak currents are ~17.1 and ~6.1% of that of the target, respectively. Thus, it is applicable to the sequence-specific sensing of NAs. The high selectivity comes from the high specificity of the PNA probe.

The practicability of this method in the sensing of NAs in complex biological matrices was studied using the spiked human serum samples, which were prepared with 10% normal human serum. As shown in Figure 5B, no obvious difference exists between the peak currents obtained in the presence of

https://doi.org/10.1021/acsami.1c17564
ACS Appl. Mater. Interfaces 2021, 13, 54794−54800

10% serum matrices (a) and those without serum matrices (b). Due to the high anti-interference capability, this method is capable of sensing NAs in complex biological matrices.

4. CONCLUSIONS

In summary, an electrochemical method has been presented for the highly selective and amplified sensing of NAs, taking advantage of a PNA recognition probe and a bioinspired electro-RAFT polymerization (BERP)-based amplification strategy. Electroreduction of the MNA organic cation, the redox center of coenzyme I, can efficiently induce the fragmentation of CPPA RAFT agents into radical species, triggering the BERP of ferrocenyl monomers, thereby recruiting plenty of Fc electroactive tags for the amplified sensing. The BERP-based strategy offers the benefits of low cost, higher labeling efficiency, improved labeling amount of polymer chains, and simple operation. Furthermore, the use of MNA as the redox mediator holds the significant advantages of low cost, high thermal stability, and milder reduction potential over coenzyme I. By virtue of the high specificity of the PNA recognition probe and the amplified signal by the BERP-based strategy, this method is highly selective (capable of sensing single-nucleotide polymorphism) and sensitive (detection limit, 0.58 fM) toward the signal-on sensing of NAs. Also, this method is capable of sensing NAs in complex serum matrices. Besides, this method holds the advantages of low sensing cost and simple operations, due to the avoidance of the synthesis and post-functionalization of nanomaterials or the bioconjugation of enzymatic labels. Taking these into account, this method shows great promise in the selective and amplified sensing of NAs.

■ ASSOCIATED CONTENT

Supporting Information

The Supporting Information is available free of charge at https://pubs.acs.org/doi/10.1021/acsami.1c17564.

Electroreduction of MNA into an organic radical; potential range of BERP; scan rate-dependent CVs; and analytical performance of various methods for NA sensing (PDF)

■ AUTHOR INFORMATION

Corresponding Authors

Qiong Hu − *Guangzhou Key Laboratory of Sensing Materials and Devices, Center for Advanced Analytical Science, School of Chemistry and Chemical Engineering, Guangzhou University, Guangzhou 510006, P. R. China;* orcid.org/0000-0001-6360-1813; Phone: +86-020-39366902; Email: q.hu@gzhu.edu.cn

Li Niu − *Guangzhou Key Laboratory of Sensing Materials and Devices, Center for Advanced Analytical Science, School of Chemistry and Chemical Engineering, Guangzhou University, Guangzhou 510006, P. R. China;* orcid.org/0000-0003-3652-2903; Phone: +86-020-39366902; Email: lniu@gzhu.edu.cn

Authors

Yilin Luo − *Guangzhou Key Laboratory of Sensing Materials and Devices, Center for Advanced Analytical Science, School of Chemistry and Chemical Engineering, Guangzhou University, Guangzhou 510006, P. R. China*

Xiaojing Cao − *Guangzhou Key Laboratory of Sensing Materials and Devices, Center for Advanced Analytical Science, School of Chemistry and Chemical Engineering, Guangzhou University, Guangzhou 510006, P. R. China*

Zhuohua Chen − *Guangzhou Key Laboratory of Sensing Materials and Devices, Center for Advanced Analytical Science, School of Chemistry and Chemical Engineering, Guangzhou University, Guangzhou 510006, P. R. China*

Yanyu Huang − *Guangzhou Key Laboratory of Sensing Materials and Devices, Center for Advanced Analytical Science, School of Chemistry and Chemical Engineering, Guangzhou University, Guangzhou 510006, P. R. China*

Complete contact information is available at: https://pubs.acs.org/10.1021/acsami.1c17564

Author Contributions

All authors have given approval to the final version of the manuscript.

Notes

The authors declare no competing financial interest.

■ ACKNOWLEDGMENTS

This work was supported by the National Natural Science Foundation of China (21904026), the start-up funding from Guangzhou University (RQ2021011), and the Innovation Training Program for College Students of Guangzhou University (S202111078031).

■ REFERENCES

(1) Allen, P. B.; Arshad, S. A.; Li, B.; Chen, X.; Ellington, A. D. DNA Circuits as Amplifiers for the Detection of Nucleic Acids on a Paperfluidic Platform. *Lab Chip* **2012**, *12*, 2951−2958.

(2) Abolhasan, R.; Mehdizadeh, A.; Rashidi, M. R.; Aghebati-Maleki, L.; Yousefi, M. Application of Hairpin DNA-Based Biosensors with Various Signal Amplification Strategies in Clinical Diagnosis. *Biosens. Bioelectron.* **2019**, *129*, 164−174.

(3) Bartold, K.; Pietrzyk-Le, A.; Golebiewska, K.; Lisowski, W.; Cauteruccio, S.; Licandro, E.; D'Souza, F.; Kutner, W. Oligonucleotide Determination via Peptide Nucleic Acid Macromolecular Imprinting in an Electropolymerized CG-Rich Artificial Oligomer Analogue. *ACS Appl. Mater. Interfaces* **2018**, *10*, 27562−27569.

(4) Jiang, J.; Lin, X.; Diao, G. Smart Combination of Cyclodextrin Polymer Host−Guest Recognition and Mg^{2+}-Assistant Cyclic Cleavage Reaction for Sensitive Electrochemical Assay of Nucleic Acids. *ACS Appl. Mater. Interfaces* **2017**, *9*, 36688−36694.

(5) Liu, L.; Yang, D.; Liu, G. Signal Amplification Strategies for Paper-Based Analytical Devices. *Biosens. Bioelectron.* **2019**, *136*, 60−75.

(6) Rajwar, D.; Ammanath, G.; Cheema, J. A.; Palaniappan, A.; Yildiz, U. H.; Liedberg, B. Tailoring Conformation-Induced Chromism of Polythiophene Copolymers for Nucleic Acid Assay at Resource Limited Settings. *ACS Appl. Mater. Interfaces* **2016**, *8*, 8349−8357.

(7) Xia, Y.; Wang, L.; Li, J.; Chen, X.; Lan, J.; Yan, A.; Lei, Y.; Yang, S.; Yang, H.; Chen, J. A Ratiometric Fluorescent Bioprobe Based on Carbon Dots and Acridone Derivate for Signal Amplification Detection Exosomal MicroRNA. *Anal. Chem.* **2018**, *90*, 8969−8976.

(8) Lai, W.; Xiao, M.; Yang, H.; Li, L.; Fan, C.; Pei, H. Circularized Blocker-Displacement Amplification for Multiplex Detection of Rare DNA Variants. *Chem. Commun.* **2020**, *56*, 12331−12334.

(9) Lei, J.; Ju, H. Signal Amplification Using Functional Nanomaterials for Biosensing. *Chem. Soc. Rev.* **2012**, *41*, 2122−2134.

(10) Lord, H.; Kelley, S. O. Nanomaterials for Ultrasensitive Electrochemical Nucleic Acids Biosensing. *J. Mater. Chem.* **2009**, *19*, 3127−3134.

(11) Melnychuk, N.; Klymchenko, A. S. DNA-Functionalized Dye-Loaded Polymeric Nanoparticles: Ultrabright FRET Platform for Amplified Detection of Nucleic Acids. *J. Am. Chem. Soc.* **2018**, *140*, 10856−10865.
(12) Miao, P.; Tang, Y.; Wang, B.; Yin, J.; Ning, L. Signal Amplification by Enzymatic Tools for Nucleic Acids. *TrAC, Trends Anal. Chem.* **2015**, *67*, 1−15.
(13) Wu, Y.; Cui, S.; Li, Q.; Zhang, R.; Song, Z.; Gao, Y.; Chen, W.; Xing, D. Recent Advances in Duplex-Specific Nuclease-Based Signal Amplification Strategies for MicroRNA Detection. *Biosens. Bioelectron.* **2020**, *165*, No. 112449.
(14) Yin, B. C.; Liu, Y. Q.; Ye, B. C. One-Step, Multiplexed Fluorescence Detection of MicroRNAs Based on Duplex-Specific Nuclease Signal Amplification. *J. Am. Chem. Soc.* **2012**, *134*, 5064−5067.
(15) Xiao, M.; Man, T.; Zhu, C.; Pei, H.; Shi, J.; Li, L.; Qu, X.; Shen, X.; Li, J. MoS_2 Nanoprobe for MicroRNA Quantification Based on Duplex-Specific Nuclease Signal Amplification. *ACS Appl. Mater. Interfaces* **2018**, *10*, 7852−7858.
(16) Hu, Q.; Gan, S.; Bao, Y.; Zhang, Y.; Han, D.; Niu, L. Controlled/"Living" Radical Polymerization-Based Signal Amplification Strategies for Biosensing. *J. Mater. Chem. B* **2020**, *8*, 3327−3340.
(17) Kim, S.; Sikes, H. D. Radical Polymerization Reactions for Amplified Biodetection Signals. *Polym. Chem.* **2020**, *11*, 1424−1444.
(18) Le Floch, F.; Ho, H. A.; Harding-Lepage, P.; Bedard, M.; Neagu-Plesu, R.; Leclerc, M. Ferrocene-Functionalized Cationic Polythiophene for the Label-Free Electrochemical Detection of DNA. *Adv. Mater.* **2005**, *17*, 1251−1254.
(19) Wu, Y.; Wei, W.; Liu, S. Target-Triggered Polymerization for Biosensing. *Acc. Chem. Res.* **2012**, *45*, 1441−1450.
(20) He, P.; Zheng, W.; Tucker, E. Z.; Gorman, C. B.; He, L. Reversible Addition−Fragmentation Chain Transfer Polymerization in DNA Biosensing. *Anal. Chem.* **2008**, *80*, 3633−3639.
(21) Hu, Q.; Wang, Q.; Sun, G.; Kong, J.; Zhang, X. Electrochemically Mediated Surface-Initiated de Novo Growth of Polymers for Amplified Electrochemical Detection of DNA. *Anal. Chem.* **2017**, *89*, 9253−9259.
(22) He, P.; Lou, X.; Woody, S. M.; He, L. Amplification-by-Polymerization in Biosensing for Human Genomic DNA Detection. *ACS Sens.* **2019**, *4*, 992−1000.
(23) Lou, X.; Lewis, M. S.; Gorman, C. B.; He, L. Detection of DNA Point Mutation by Atom Transfer Radical Polymerization. *Anal. Chem.* **2005**, *77*, 4698−4705.
(24) Boyer, C.; Bulmus, V.; Davis, T. P.; Ladmiral, V.; Liu, J.; Perrier, S. Bioapplications of RAFT Polymerization. *Chem. Rev.* **2009**, *109*, 5402−5436.
(25) Chiefari, J.; Chong, Y. K.; Ercole, F.; Krstina, J.; Jeffery, J.; Le, T. P. T.; Mayadunne, R. T. A.; Meijs, G. F.; Moad, C. L.; Moad, G.; Rizzardo, E.; Thang, S. H. Living Free-Radical Polymerization by Reversible Addition−Fragmentation Chain Transfer: the RAFT Process. *Macromolecules* **1998**, *31*, 5559−5562.
(26) Perrier, S. 50th Anniversary Perspective: RAFT Polymerization—A User Guide. *Macromolecules* **2017**, *50*, 7433−7447.
(27) Moad, G.; Chen, M.; Häussler, M.; Postma, A.; Rizzardo, E.; Thang, S. H. Functional Polymers for Optoelectronic Applications by RAFT Polymerization. *Polym. Chem.* **2011**, *2*, 492−519.
(28) Hu, Q.; Han, D.; Gan, S.; Bao, Y.; Niu, L. Surface-Initiated-Reversible-Addition−Fragmentation-Chain-Transfer Polymerization for Electrochemical DNA Biosensing. *Anal. Chem.* **2018**, *90*, 12207−12213.
(29) Zhang, B.; Wang, X.; Zhu, A.; Ma, K.; Lv, Y.; Wang, X.; An, Z. Enzyme-Initiated Reversible Addition−Fragmentation Chain Transfer Polymerization. *Macromolecules* **2015**, *48*, 7792−7802.
(30) Li, S.; Han, G.; Zhang, W. Photoregulated Reversible Addition−Fragmentation Chain Transfer (RAFT) Polymerization. *Polym. Chem.* **2020**, *11*, 1830−1844.
(31) McKenzie, T. G.; Colombo, E.; Fu, Q.; Ashokkumar, M.; Qiao, G. G. Sono-RAFT Polymerization in Aqueous Medium. *Angew. Chem., Int. Ed.* **2017**, *56*, 12302−12306.
(32) Hu, Q.; Kong, J.; Han, D.; Zhang, Y.; Bao, Y.; Zhang, X.; Niu, L. Electrochemically Controlled RAFT Polymerization for Highly Sensitive Electrochemical Biosensing of Protein Kinase Activity. *Anal. Chem.* **2019**, *91*, 1936−1943.
(33) Hu, Q.; Su, L.; Chen, Z.; Huang, Y.; Qin, D.; Niu, L. Coenzyme-Mediated Electro-RAFT Polymerization for Amplified Electrochemical Interrogation of Trypsin Activity. *Anal. Chem.* **2021**, *93*, 9602−9608.
(34) Wang, Y.; Fantin, M.; Park, S.; Gottlieb, E.; Fu, L.; Matyjaszewski, K. Electrochemically Mediated Reversible Addition−Fragmentation Chain-Transfer Polymerization. *Macromolecules* **2017**, *50*, 7872−7879.
(35) Lorandi, F.; Fantin, M.; Shanmugam, S.; Wang, Y.; Isse, A. A.; Gennaro, A.; Matyjaszewski, K. Toward Electrochemically Mediated Reversible Addition−Fragmentation Chain-Transfer (*e*RAFT) Polymerization: Can Propagating Radicals Be Efficiently Electrogenerated from RAFT Agents? *Macromolecules* **2019**, *52*, 1479−1488.
(36) Strover, L. T.; Postma, A.; Horne, M. D.; Moad, G. Anthraquinone-Mediated Reduction of a Trithiocarbonate Chain-Transfer Agent to Initiate Electrochemical Reversible Addition−Fragmentation Chain Transfer Polymerization. *Macromolecules* **2020**, *53*, 10315−10322.
(37) Sang, W.; Xu, M.; Yan, Q. Coenzyme-Catalyzed Electro-RAFT Polymerization. *ACS Macro Lett.* **2017**, *6*, 1337−1341.
(38) Schmakel, C. O.; Santhanam, K. S. V.; Elving, P. J. Nicotinamide Adenine Dinucleotide (NAD^+) and Related Compounds. Electrochemical Redox Pattern and Allied Chemical Behavior. *J. Am. Chem. Soc.* **1975**, *97*, 5083−5092.
(39) Santhanam, K. S. V.; Elving, P. J. Electrochemical Redox Pattern for Nicotinamide Species in Nonaqueous Media. *J. Am. Chem. Soc.* **1973**, *95*, 5482−5490.
(40) Wang, J.; Palecek, E.; Nielsen, P. E.; Rivas, G.; Cai, X.; Shiraishi, H.; Dontha, N.; Luo, D.; Farias, P. A. M. Peptide Nucleic Acid Probes for Sequence-Specific DNA Biosensors. *J. Am. Chem. Soc.* **1996**, *118*, 7667−7670.
(41) Hu, Q.; Su, L.; Huang, Y.; Chen, Z.; Cao, X.; Luo, Y.; Dongdong, Qin.; Niu, L. Coenzyme-Mediated Electro-Grafting for Ultrasensitive Electrochemical DNA Biosensing. *Sens. Actuators, B* **2021**, *346*, No. 130551.
(42) Huang, M.; Zhou, X.; Wang, H.; Xing, D. Clustered Regularly Interspaced Short Palindromic Repeats/Cas9 Triggered Isothermal Amplification for Site-Specific Nucleic Acid Detection. *Anal. Chem.* **2018**, *90*, 2193−2200.
(43) Zhang, S.; Wang, K.; Li, K. B.; Shi, W.; Jia, W. P.; Chen, X.; Sun, T.; Han, D. M. A DNA-Stabilized Silver Nanoclusters/Graphene Oxide-Based Platform for the Sensitive Detection of DNA through Hybridization Chain Reaction. *Biosens. Bioelectron.* **2017**, *91*, 374−379.
(44) Xiao, M.; Chandrasekaran, A. R.; Ji, W.; Li, F.; Man, T.; Zhu, C.; Shen, X.; Pei, H.; Li, Q.; Li, L. Affinity-Modulated Molecular Beacons on MoS_2 Nanosheets for MicroRNA Detection. *ACS Appl. Mater. Interfaces* **2018**, *10*, 35794−35800.
(45) Liu, P. F.; Zhao, K. R.; Liu, Z. J.; Wang, L.; Ye, S. Y.; Liang, G. X. Cas12a-Based Electrochemiluminescence Biosensor for Target Amplification-Free DNA Detection. *Biosens. Bioelectron.* **2021**, *176*, No. 112954.
(46) Faria, H. A. M.; Zucolotto, V. Label-Free Electrochemical DNA Biosensor for Zika Virus Identification. *Biosens. Bioelectron.* **2019**, *131*, 149−155.
(47) Fu, P.; Xing, S.; Xu, M.; Zhao, Y.; Zhao, C. Peptide Nucleic Acid-Based Electrochemical Biosensor for Simultaneous Detection of Multiple MicroRNAs from Cancer Cells with Catalytic Hairpin Assembly Amplification. *Sens. Actuators, B* **2020**, *305*, No. 127545.
(48) Xiong, E.; Yan, X.; Zhang, X.; Liu, Y.; Zhou, J.; Chen, J. Exonuclease III−Assisted Cascade Signal Amplification Strategy for Label-Free and Ultrasensitive Electrochemical Detection of Nucleic Acids. *Biosens. Bioelectron.* **2017**, *87*, 732−736.
(49) Zhou, L.; Wang, T.; Bai, Y.; Li, Y.; Qiu, J.; Yu, W.; Zhang, S. Dual-Amplified Strategy for Ultrasensitive Electrochemical Biosensor

Based on Click Chemistry-Mediated Enzyme-Assisted Target Recycling and Functionalized Fullerene Nanoparticles in the Detection of MicroRNA-141. *Biosens. Bioelectron.* **2020**, *150*, No. 111964.
(50) Long, D.; Li, M.; Wang, H.; Wang, H.; Chai, Y.; Yuan, R. A Photoelectrochemical Biosensor Based on Fullerene with Methylene Blue as a Sensitizer for Ultrasensitive DNA Detection. *Biosens. Bioelectron.* **2019**, *142*, No. 111579.
(51) Zang, Y.; Lei, J.; Hao, Q.; Ju, H. CdS/MoS_2 Heterojunction-Based Photoelectrochemical DNA Biosensor via Enhanced Chemiluminescence Excitation. *Biosens. Bioelectron.* **2016**, *77*, 557−564.

https://doi.org/10.1021/acsami.1c17564
ACS Appl. Mater. Interfaces 2021, 13, 54794−54800